CILAMCE 2017
Florianópolis - Santa Catarina - Brazil

INFLUENCE OF CONSTITUTIVE RELATIONS ON THE ANALYSIS OF STRUTUCTURAL ELEMENTS IN CONCRETE WITH STRONG DISCONTINUITIES

Cristiane Zuffo da Silva Marasca

cristiane.zuffo@gmail.com

Universidade Paranaense

Avenida Júlio Assis Cavalheiro n. 2000, 85601-000, Francisco Beltrão, Paraná, Brasil

Virgínia Maria Rosito d'Ávila Bessa

Eduardo Bittencourt

vichy@ufrgs.br

eduardo.bittencourt@ufrgs.br

Universidade Federal do Rio Grande do Sul

Avenida Osvaldo Aranha n. 99, 3 andar, 90035-190, Porto Alegre, Rio Grande do Sul, Brasil

Abstract. *The influence of different constitutive relations on the structural analysis of concrete elements is studied. In concrete, as the maximum principal stress exceeds the tensile strength, cracks open in perpendicular planes to this stress. In order to analyze the behavior of the cracked material, a statically and kinematically optimal non-symmetric formulation (SKON) is used. The influence of two constitutive relations of stress versus crack opening was analyzed to represent the behavior of the material after reaching tensile strength. The linear constitutive relation was not suitable because overestimates the maximum stress and presents a more brittle softening branch. In contrast, the exponential model proved to be quite efficien, representing the behavior of quasi- brittle materials. The validation of the results is performed by tests in concrete elements.*

Keywords: *Strong discontinuities, Constitutive relations, Concrete, Elemental enrichments*

1 INTRODUCTION

In quasi-brittle materials, the appearance and propagation of cracks happens due to the formation of zones with strain localization where the concentration of damage and other inelastic effects occurs. Crack propagation occurs in arbitrary directions that can be influenced by the geometry of the structure, boundary conditions, heterogeneity or local defects of the material (Driemeier, 1999).

In concrete, an almost linear elastic behavior occurs before peak stress. When reaching the maximum principal stress, the location of deformations happens and the crack opens in planes perpendicular to this stress (D'Hers; Dvorkin, 2008). In the post-peak branch, the stress decrease and the regions with and without crack present different behaviors. In the cracked zone occurs an increase of deformations and in the region without cracks, a shrinkage occurs. This phenomenon was first observed by Hillerborg, Modéer and Petersson (1976).

Since the material no longer behaves evenly, two curves are required to represent the post-peak behavior of the material: a stress-strain curve for the part of the material undergoing elastic discharge and a transmitted stresses *versus* crack opening curve in the softening branch (Araújo, 2001). According to Lens (2009), the constitutive relation adopted in the post-peak have an effect on the softening behavior and maximum load reached.

Among several transmitted stresses *versus* crack opening relations that can be used to represent the post-peak branch, in this work we will verify the influence of a linear relation and an exponential relation in the representation of post-peak concrete behavior.

The model implemented belongs to the strong discontinuities models and was proposed by Dvorkin, Cuitiño and Gioia (1990). The model is nonsymmetrical (SKON) according to the nomenclature of Jirásek (2000) and is classified as elemental enrichment elements (E-FEM).

The outline of the rest of this paper is as follows. Section 2 presents the Variational Principle governing the problem and describes the asymmetric model implemented. Section 3 provides the constitutive relations. Section 4 shows the numerical examples and the conclusions are discussed in chapter 5.

2 STRONG DISCONTINUITY MODEL

The strong discontinuity models simulate the relation between forces through the crack and the opening of the crack (discontinuity of the internal displacement field of the element). For these models, the Variational Principle that represent the problem needs to include the relation between the transmitted stresses *versus* crack opening (d'Ávila, 2003).

In the implemented model (Dvorkin, Cuitiño, Gioia, 1990), the Hu-Washizu Variational Principle that incorporates the discontinuities in the displacement field is used. In this principle the displacement, $\mathbf{u}$, strain, $\boldsymbol{\varepsilon}$, and stress, $\boldsymbol{\sigma}$, fields are independent of each other. These fields are defined in a $\mathbf{V}$ domain, where volume forces, $\hat{\mathbf{b}}$, are applied. The surface is divided into two parts: $\mathbf{S_u}$, where the essential boundary conditions, $\mathbf{u} = \hat{\mathbf{u}}$, are applied; and $\mathbf{S_t}$, in which the natural boundary conditions are applied (Figure 1a) (Jirásek, 2000).

Proceedings of the XXXVIII Iberian Latin-American Congress on Computational Methods in Engineering
P.O. Faria, R.H. Lopez, L.F.F. Miguel, W.J.S. Gomes, M. Noronha (Editores), ABMEC, Florianópolis, SC, Brazil, November 5-8, 2017.

The Principle can be extended to a body with an internal interface **S**, Figure 1b), which divides the domain and the boundary conditions into two parts. A field of surface forces, $\mathbf{t_j}$, appears on the inner surface. This field is a function of the discontinuity of displacements through the internal interface (d'Ávila, 2003).

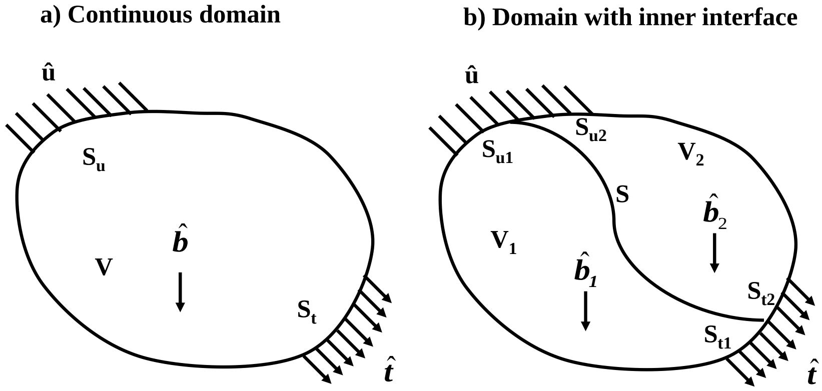

Figure 1: Boundary condition in the domain. a) continuous, b) with inner interface.

The field equations that govern the problem can be coupled on a Variational Principle according to Eq. (1)

$$\int_V \delta\boldsymbol{\varepsilon}^T \tilde{\boldsymbol{\sigma}}(\boldsymbol{\varepsilon})\, dV + \delta \int_V \boldsymbol{\sigma}^T \left(\nabla \mathbf{u} - \boldsymbol{\varepsilon}\right) dV = \int_{St} \delta\mathbf{u}^T \hat{\mathbf{t}}\, dS + \int_V \delta\mathbf{u}^T \hat{\mathbf{b}}\, dV, \tag{1}$$

in which δ represents variation, $\tilde{\boldsymbol{\sigma}}(\boldsymbol{\varepsilon})$ the stress obtained from the constitutive relations, $\nabla\mathbf{u}$ the displacement gradient.

The numerical modeling of strong discontinuities on solids requires the use of a formulation that correctly represents the discontinuity in the displacement field, considering the independence between the fields of stress, strain and displacement. A general formulation in the context of finite elements can be found on the works of Jirásek (2000) and Spencer (2000).

According to Jirásek (2000), the general formulation can be particularized in three cases: Kinematically optimal symmetric elements (KOS), Statically optimal symmetric elements (SOS), Kinematically and statically optimal non-symmetric elements (SKON). The first describes the kinematic aspects satisfactorily, but leads to an inappropriate relation of stresses in the crack, the second considers the continuity of stresses through the internal interface, but does not guarantee kinematic continuity and the latter presents a better performance by using a continuity condition of natural stresses and fairly well represent kinematic continuity.

A kinematically and statically optimal non-symmetric elements (SKON) model is implemented because this formulation presents more robust and reliable results than the others (Oliver, Huespe, Samaniego, 2003), for more information see (Silva, 2015).

2.1 Asymmetric model implemented

In this paper an asymmetric model proposed by Dvorkin, Cuitiño and Gioia (1990) was implemented to represent the strong discontinuities, with the following characteristics:

a) consider the entire element as a minimum domain in the localization of strains, instead of working at the integration point level.

b) the strain localization within the finite element is considered as a displacement discontinuity line incorporated in the element domain.

c) two constitutive relations are defined to represent the material behavior when the localization is started at element. A stress-displacement relation for the discontinuity line, related to fracture energy, and a stress-strain relation for the element domain.

d) the elements resulting from this formulation are non-conforming.

e) this formulation represents the global effects of locating strains on a structure. Hence, it is not possible to obtain a detailed description of the stress field near the localization zone

In order to better understand the implemented asymmetric formulation, we initially analyze the simple case of a bar finite element with two nodes, Figure 2a).

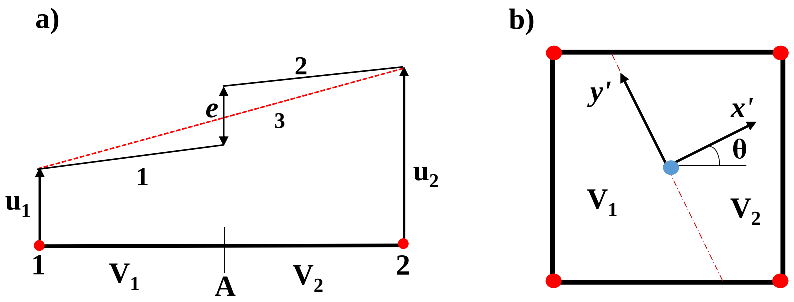

Figure 2: Finite element whit localization line a) one-dimensional b) two-dimensional

Before the opening of the cracks the displacements are obtained according to Eq. (2).

$$\mathbf{u} \approx \mathbf{NU}, \tag{2}$$

where **U** is the vector that contains the increments of nodal displacement and **N** contains the interpolation functions.

The dashed line 3 in the Figure 2a) represents this interpolation. When the crack opens a discontinuity of displacements is considered in center *A*, which divides the element into two subdomains V_1 and V_2. It is assumed that V_2 suffers an increment of rigid body displacement (**e**) regarding V_1.

In order to obtain the same strain for both subdomains, the interpolations of lines 1 and 2 shown in Figure 2a) are adopted for V_1 and V_2. Therefore, the displacements for each subdomain considering the line of discontinuity becomes

$$\mathbf{u}_1 = \mathbf{N}\left(\mathbf{U} - \phi\mathbf{e}\right) \tag{3}$$

and

$$\mathbf{u}_2 = \mathbf{N}\left(\mathbf{U} - \phi\mathbf{e}\right) + \mathbf{e}. \tag{4}$$

Being $\boldsymbol{\phi} = \begin{pmatrix} 0 & 1 \end{pmatrix}^T$. Deriving the Eqs. (3) and (4), the same incremental strain is obtained. Therefore, for any point V_1 and V_2

$$\boldsymbol{\varepsilon} = \mathbf{B}\left(\mathbf{U} - \boldsymbol{\phi}\mathbf{e}\right). \tag{5}$$

For the two-dimensional case (Figure 2b) the concepts presented above can be generalized considering

$$\mathbf{e} = \mathbf{d_c} = \mathbf{Re}', \tag{6}$$

where **e'** contains the rigid body motion components associated with the localization line, evaluated at the center of the element, in the local system (*x', y'*)

$$\mathbf{e}' = \begin{bmatrix} u^c \\ v^c \end{bmatrix}, \tag{7}$$

and ***R*** is the rotation matrix of the local Cartesian system of discontinuity (*x', y'*) to the coordinate system of the element. Moreover, $\boldsymbol{\phi}$ becomes a matrix defined by

$$\boldsymbol{\phi} = \begin{bmatrix} \boldsymbol{\phi}_1 & \boldsymbol{\phi}_2 & \boldsymbol{\phi}_3 & \boldsymbol{\phi}_4 \end{bmatrix}^T, \tag{8}$$

where each submatrix $\boldsymbol{\phi}_\mathrm{n}$ is a matrix of 2x2 dimension, defined according to

$$\boldsymbol{\phi}_n = \begin{cases} \mathbf{0} \text{ em } \mathrm{V}_1 \\ \mathbf{I} \text{ em } \mathrm{V}_2 \end{cases} \tag{9}$$

where **I** represents the identity matrix.

Therefore, the displacements $\mathbf{u_1}$ and $\mathbf{u_2}$ takes the form.

$$\mathbf{u_1} = \mathbf{N}\left(\mathbf{U} - \boldsymbol{\phi}\mathbf{Re}'\right) \tag{10}$$

and

$$\mathbf{u_2} = \mathbf{N}\left(\mathbf{U} - \boldsymbol{\phi}\mathbf{Re}'\right) + \mathbf{Re}', \tag{11}$$

where

$$\mathbf{d_N} = \mathbf{U} - \boldsymbol{\phi}\mathbf{Re}', \tag{12}$$

which is the displacement that causes strains.

For two points near the line of discontinuity, one on V_1 and another on V_2, the displacement is given by

$$\mathbf{u}^{+} - \mathbf{u}^{-} = \mathbf{R}\mathbf{e}'. \tag{13}$$

The strain for the two-dimensional case is

$$\boldsymbol{\varepsilon} = \mathbf{B}\left(\mathbf{U} - \boldsymbol{\phi}\mathbf{R}\mathbf{e}'\right) = \mathbf{B}\mathbf{d}_{\mathbf{N}}. \tag{14}$$

After the crack is open, it is necessary to consider an internal equilibrium condition for the discontinuity line. Considering the Eq. (1), see more details in (Silva, 2015), we have

$$\int_{S_L} \mathbf{t}dS = \int_{S_L} \mathbf{P}^T \boldsymbol{\sigma} dS. \tag{15}$$

The matrix **P** selects the stress components that will be transmitted through the crack.

The constitutive relation for the localization line is defined as

$$\mathbf{t} = \mathbf{D}^{cr}\mathbf{e}' \tag{16}$$

$$\begin{bmatrix} t_1 \\ t_2 \end{bmatrix} = \begin{bmatrix} E_t\left(u^c\right) & 0 \\ 0 & G_t \end{bmatrix} \begin{bmatrix} u^c \\ v^c \end{bmatrix}, \tag{17}$$

where E_t (u^c) is adjusted according to the fracture *energy,* G_f*, and* G_t is related to the shear modulus.

For the element domain

$$^{t+\Delta t}\boldsymbol{\sigma} = {}^{t}\boldsymbol{\sigma} + \mathbf{D}^{e}\Delta\boldsymbol{\varepsilon} \tag{18}$$

In that t and $t+\Delta t$ represents pseudo-times relatives to the load increments, where t is the previous increment and $t+\Delta t$ is the current load increment (total). $\mathbf{D}^{\mathbf{e}}$ is the elastic constitutive matrix of the material.

For the elements in the region where the localization does not occur, the same relation presented in (18) is used.

Starting from Eq. (1), considering the strain in Eq. (14) e stress in Eq. (18) the global system become (see the complete formulation in Silva (2015)):

$$\int_{V} \mathbf{B}^T \mathbf{D}^e \mathbf{B}\left(\mathbf{U} - \boldsymbol{\phi}\mathbf{R}\mathbf{e}'\right) dV = {}^{t+\Delta t}\mathbf{f}_{\mathbf{ext}} - {}^{t}\mathbf{F}. \tag{19}$$

Where

$$^{t+\Delta t}\mathbf{f}_{\mathbf{ext}} = \int_{S} \mathbf{N}^T \, {}^{t+\Delta t}\mathbf{p} dS \tag{20}$$

and

$$
{}^{t}\mathbf{F} = \int_{V} \mathbf{B}^{T}\,{}^{t}\boldsymbol{\sigma} dV. \tag{21}
$$

Replacing (18) and (16) in the additional equilibrium condition (15), we have

$$
\left(\int_{S_L} \mathbf{P}^{T}\mathbf{D}^{e}\mathbf{B} dS \right)\mathbf{U} = \left[\int_{S_L} \left(\mathbf{P}^{T}\mathbf{D}^{e}\mathbf{B}\boldsymbol{\phi}\mathbf{R} + \mathbf{D}^{cr} \right) dS \right]\mathbf{e}' \tag{22}
$$

where

$$
\mathbf{S}_{\mathbf{uu}} = \int_{S_L} \mathbf{P}^{T}\mathbf{D}^{e}\mathbf{B} dS \tag{23}
$$

and

$$
\mathbf{S}_{\mathbf{cc}} = \int_{S_L} \left(\mathbf{P}^{T}\mathbf{D}^{e}\mathbf{B}\boldsymbol{\phi}\mathbf{R} + \mathbf{D}^{cr} \right) dS \tag{24}
$$

Therefore, replacing (23) and (24) in (22) and isolating the additional displacement, we obtain

$$
\mathbf{e}' = \mathbf{S}_{\mathbf{cc}}^{-1}\mathbf{S}_{\mathbf{uu}}\mathbf{U} \tag{25}
$$

From (25) we have the condensation of the internal degrees of freedom of Eq.(19) resulting in

$$
\left[\int_{V} \mathbf{B}^{T}\mathbf{D}^{e}\mathbf{B}\left(\mathbf{I} - \boldsymbol{\phi}\mathbf{R}\mathbf{S}_{\mathbf{cc}}^{-1}\mathbf{S}_{\mathbf{uu}} \right) dV \right]\mathbf{U} = {}^{t+\Delta t}\mathbf{f}_{\mathbf{ext}} - {}^{t}\mathbf{F} \tag{26}
$$

where

$$
{}^{t}\mathbf{K}^{*} = \int_{V} \mathbf{B}^{T}\mathbf{D}^{e}\mathbf{B}\left(\mathbf{I} - \boldsymbol{\phi}\mathbf{R}\mathbf{S}_{\mathbf{cc}}^{-1}\mathbf{S}_{\mathbf{uu}} \right) dV \tag{27}
$$

is the consistent tangent stiffness matrix. It is observed that the terms in parentheses make the matrix asymmetric, which can be a problem for implementation in pre-existing codes that use only symmetric matrices.

In the implemented model, only the symmetric part of the stiffness matrix of Eq. (27) was used because, for the analyzed problems, the difference in disregarding the asymmetric part is irrelevant. This is supported by Dvorkin, Cuitiño and Gioia (1990), in which it was observed that although it required more iterations to achieve convergence the symmetric matrix presented satisfactory results. Although using only the symmetrical part of the stiffness matrix in Eq. (27), the presented method produces results more consistent and robust than methods based on the symmetrical formulations. Considering that in the propagation of cracks the conditions of continuity of stresses at the internal interface and rigid body motion between the sides of the element separated by the crack are still guaranteed.

Therefore, at the global level the system of equations to be solved is given by Eq. (28)

$$ {}^{t}\mathbf{K}^{*}\mathbf{U} = {}^{t+\Delta t}\mathbf{f}_{\mathbf{ext}} - {}^{t}\mathbf{F}. \tag{28} $$

To obtain the equilibrium at time $t+\Delta t$ it is necessary to iterate at the element level the Eq. (15) and, at the global level (structure), using load control for the i_{th} iteration:

$$ \begin{aligned} {}^{t}\mathbf{K}^{*}\Delta\mathbf{U}^{(i)} &= {}^{t+\Delta t}\mathbf{f}_{\mathbf{ext}} - {}^{t}\mathbf{F}^{(i-1)} \\ \mathbf{U}^{(i)} &= \mathbf{U}^{(i-1)} + \Delta\mathbf{U}^{(i)} \end{aligned} \tag{29} $$

The final equilibrium of the equations given in Eq. (29) is obtained using the Newton-Rhapson iterative method.

The stiffness matrix is obtained by integration with 2x2 Gauss points. After the crack opens on an element, the element is considered as the minimum domain, i.e., all properties are calculated in the center of the element, using integration with 1 Gauss point. This may lead to null strains modes (spurious modes) in the use of distorted finite elements in the cracked region. In order to avoid this problem, it is interesting to use finite elements able to overcome this problem, such as the QMITC element (d’Ávila, 2003).

To obtain the equilibrium within the element, Eq. (15), presents some particularities. Dvorkin and Assanelli (1991) show an algorithm to obtain this equilibrium when a localization line is opened inside an element:

a) consider the crack opening equal to the opening of the previous global iteration

$k = 0$ local iteration counter

$$ {}^{t+\Delta t}\mathbf{e}'^{(i)}_{(0)} = {}^{t}\mathbf{e}' \tag{30} $$

b) from the displacement obtained by the global equation system, determine the displacement that causes strain in the element

$$ {}^{t+\Delta t}\mathbf{d}_{\mathbf{Ne}(k)}^{(i)} = {}^{t+\Delta t}\mathbf{U}^{(i)} - {}^{t+\Delta t}\boldsymbol{\phi}\mathbf{R}\mathbf{e}'^{(i)}_{(k)} \tag{31} $$

c) calculate the incremental stress in the element domain, using (18)

d) calculate the incremental stress in the discontinuity line using (16)

e) obtain the increment of crack opening

$$ \Delta\mathbf{e}'^{(i)}_{(k)} = \mathbf{S}_{\mathbf{cc}}^{-1}\left[\int_{S_L}\mathbf{P}^{T}\boldsymbol{\sigma}^{(i)}_{(k)}dS - \int_{S_L}\mathbf{t}^{(i)}_{(k)}dS\right] \tag{32} $$

f) update the crack opening value

Proceedings of the XXXVIII Iberian Latin-American Congress on Computational Methods in Engineering
P.O. Faria, R.H. Lopez, L.F.F. Miguel, W.J.S. Gomes, M. Noronha (Editores), ABMEC, Florianópolis, SC, Brazil, November 5-8, 2017.

$$ {}^{t+\Delta t}\mathbf{e}'^{(i)}_{(k+1)} = {}^{t+\Delta t}\mathbf{e}'^{(i)}_{(k)} + \Delta\mathbf{e}'^{(i)}_{(k)} \tag{33}$$

g) verify convergence

$$ \text{if } \left(\left|\Delta\mathbf{e}'\right| < Tolerance\right) \text{ ok} \tag{34}$$

h) else

$$ k = k + 1 \tag{35}$$

i) return to item b)

3 CONSTITUTIVE RELATIONS

Quasi-brittle materials, such as concrete, present a linear behavior until certain levels of loading. For higher levels of loading, a non-elastic regime precedes the rupture (Driemeier, 1999). Generally, in this type of material, the change of behavior is observed when the maximum principal stress exceeds the tensile strength. From this point, in the cracked region occurs an increase of strain, represented by curve II of Fig. 3. Because of this process, in the region without crack, a shrinkage occurs, the phenomenon is observed in curve I of Fig. 3. This phenomenon was first observed by Hillerborg, Modéer, Petersson (1976).

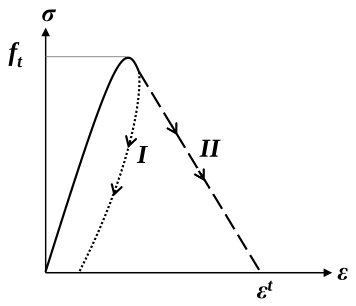

Figure 3: Behavior of regions without (I) and with (II) crack

In the post-peak constitutive relation for a cracked zone (transmitted stress (**σ**) *versus* crack opening (***w***)) the specific fracture energy (***G$_f$***) is represented by the area under the curve. According to Lens (2009), the constitutive relation adopted in the post-peak have an effect on the softening behavior and maximum load reached . The constitutive relations used in this work are presented in Fig 4.

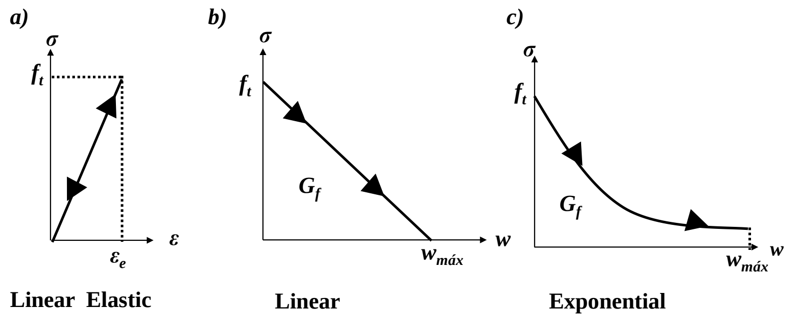

Figure 4: Constitutive relations: a) linear elastic; b) linear softening; c) exponential softening

The linear elastic constitutive relation (Fig. 4a) is used to represent the behavior of the intact material (without cracking) and to represent the discharge behavior of the material in the non-cracked region after the cracking process has begun. This relation is presented in Eq. (36).

$$\boldsymbol{\sigma} = \mathbf{D}^{e}\boldsymbol{\varepsilon}, \tag{36}$$

where $\boldsymbol{\sigma}$ represents the stress in the domain, $\mathbf{D}^{\mathbf{e}}$ represents the elastic constitutive matrix and $\boldsymbol{\varepsilon}$ represents the strain.

The linear softening constitutive relation, Fig. 4b), used for the cracked line is the Hillerborg model (Hillerborg, Modéer, Petersson, 1976). The area under the graphic in the Fig. 4b) represents the fracture energy.

The fracture energy and tensile strength are characteristic of the material, then the maximum crack opening can be obtained through Eq. (37),

$$w_{\max} = \frac{2G_f}{f_t}. \tag{37}$$

The Eq. (38) represents this constitutive relation.

$$\sigma = f_t\left(1 - \frac{w}{w_{máx}}\right) \tag{38}$$

The exponential softening constitutive relation, schematized in Fig. 4c) is based on the model presented by Dvorkin, Cuitiño and Gioia (1990). The Eqs. (39) and (40) represent the exponential softening curve

$$\sigma = f_t \exp(-aw) \tag{39}$$

$$a = \alpha f_t / G_f \tag{40}$$

A limit is imposed for the factor exp (-aw) = 0.05 in order to obtain a maximum crack opening value ($w_{máx}$). In addition, in the Dvorkin model the factor α is taken as 0.95 and in the

Proceedings of the XXXVIII Iberian Latin-American Congress on Computational Methods in Engineering
P.O. Faria, R.H. Lopez, L.F.F. Miguel, W.J.S. Gomes, M. Noronha (Editores), ABMEC, Florianópolis, SC, Brazil, November 5-8, 2017.

current model a value of 1.05 was used in order to better represent the overall behavior of the structure with this value.

4 NUMERICAL EXAMPLES

In this section, we present the numerical experiments to illustrate the application of the presented methodology and analyze the influence of the constitutive relations in the post-peak branch.

4.1 Pure Tensile Test

This simulation has the purpose of analyze the influence of the structure length on the material behavior, besides the influence of the constitutive relation. Figure 5 shows the boundary conditions of the problem.

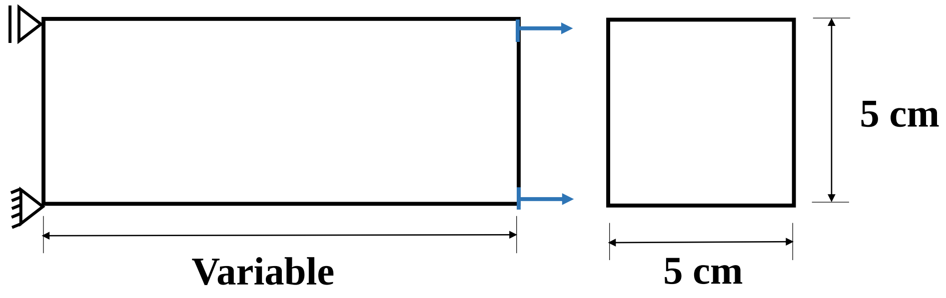

Figure 5: pure tensile test – geometry and boundary conditions

Table 1 shows the input data used for the example developed. These values were obtained from d'Avila (2003).

Table 1. Input parameters - Tensile with length variation

Geometric Properties	
Length	10,50,100,125,150 cm
Height	5 cm
Thickness	5 cm
Material Properties	
Tensile strength (ft)	0.158 kN/cm²
Young Modulus (E)	3224 kN/cm²
Poisson coefficient (ν)	0.0
Fracture energy (Gf)	4.87E-4 kN/cm

For the analysis of the length influence we used the linear model proposed by Hillerborg (Hillerborg, Modéer, Petersson, 1976) for the post-peak branch. Figure 6 shows the relation between the stress and the total displacement obtained. As can be observed, the behavior becomes brittle with length increasing. The structures with length of 10 centimeters, 50 centimeters and 100 centimeters have a post-peak behavior with softening. The 125 centimeters structure has a totally brittle behavior. The 150 centimeters structure shows a reduction in displacements after reaching tensile strength, a phenomenon known as snapback. This phenomenon can be observed experimentally with the increase of the structure length, as in the work of Hordijk (1991). It is important to note that in this work the snapback effect was not obtained numerically, the dashed line only indicates the theoretical solution.

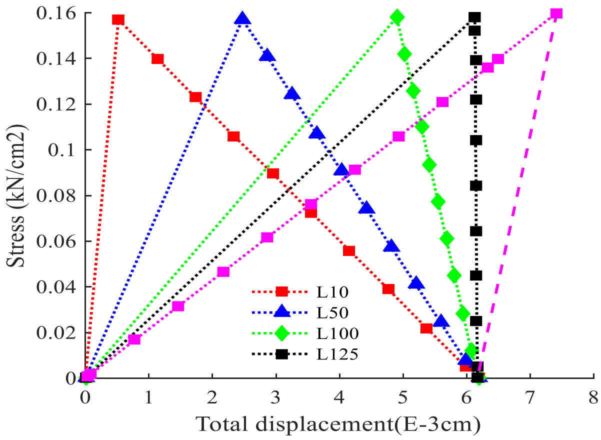

Figure 6: Stress *versus* displacement

The variation of the behavior due to the length of the structures can be analyzed through the concepts of material strength and fracture mechanics. It is known that before reaching tensile strength the material exhibits a linear elastic behavior, so the displacement can be given by Eq. (41),

$$u = \frac{FL}{AE}. \tag{41}$$

Where u is the displacement of transversal section, F is the applied force, L is the length of structure, A is the area of transversal section and E is the Young Modulus.

From Eq. (41) , it is observed that the displacement is dependent on the length of the structure for the same applied force. Thus, assuming the application of a load on all structures that leads to the tensile strength, the displacement will increase linearly with the size of the structure, as can be seen in Fig. 6.

When the applied load exceeds the tensile strength, two simultaneous processes occur: crack opening and the strain reduction in non-cracked region. Therefore, at the end of the process, when it is no more possible to transfer stresses through the crack, displacement (u) will be equal to the maximum crack opening ($w_{máx}$), according to Eq. (42)

$$u = w_{\text{máx}} \tag{42}$$

We can conclude that all the structures will have the same final displacement, since the properties of the material are the same and so will have the same crack opening. In this case, what determines the quasi-brittle or brittle behavior of the material is the displacement that occurs in the elastic regime of the material.

Figure 7 shows the softening models employed. Note that in the linear softening model the maximum crack opening is smaller than in the exponential model. As will be seen later this difference in behavior will affect the overall response of the structure.

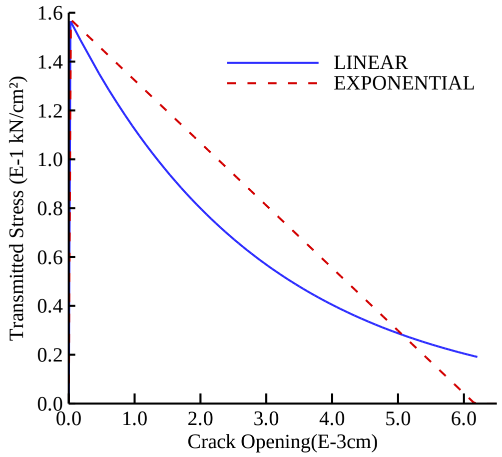

Figure 7: softening models employed

Figure 8 shows the relation between the stress and total deformation of the structure, i.e. the deformation relative to the total displacement of the free end.

a)

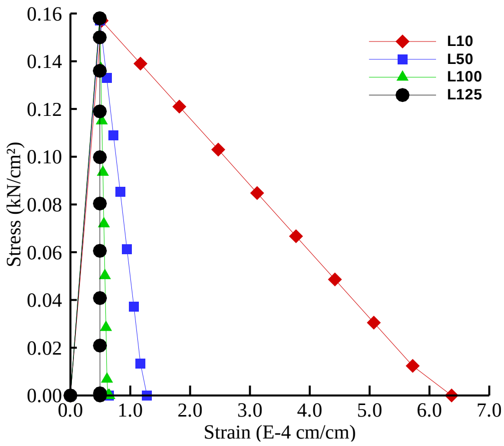

b)

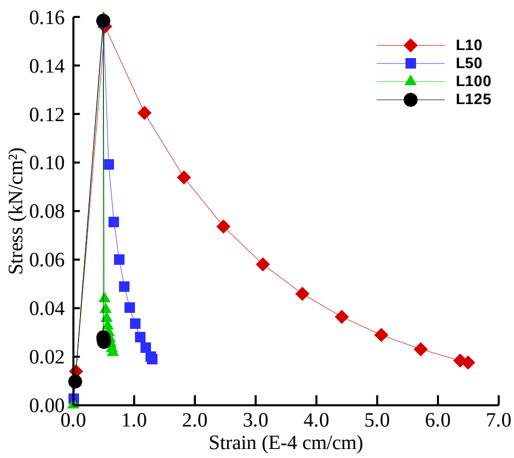

Figure 8: Stress versus Total strain. a) linear model. b) exponential model

It can be seen from Fig.8 that shorter structures present more strain after the cracks open than longer structures, representing the increase of the fragility with the increase of the length of the structure. In this figure the results are not presented for the length 150 centimeters because it was not possible to simulate the softening branch of this structure.

Several experimental analyzes for concrete elements under tensile shows an exponential behavior of the concrete in the post-peak branch, e.g., Hordjk (1991) and (Van Vliet, Van Mier, 2000). Thus, the data obtained in Fig. 8b) represent more realistic results than that obtained in Fig. 8a).

4.2 Bending test

A classic test to analyze the crack propagation in mode I is the notched beam tested under three-point bending. In this paper, the beam tested experimentally by Petersson (1981) was used as reference.

Figure 9 shows the beam geometry and the boundary conditions. The beam was discretized with three different finite element meshes, according to Table 2.

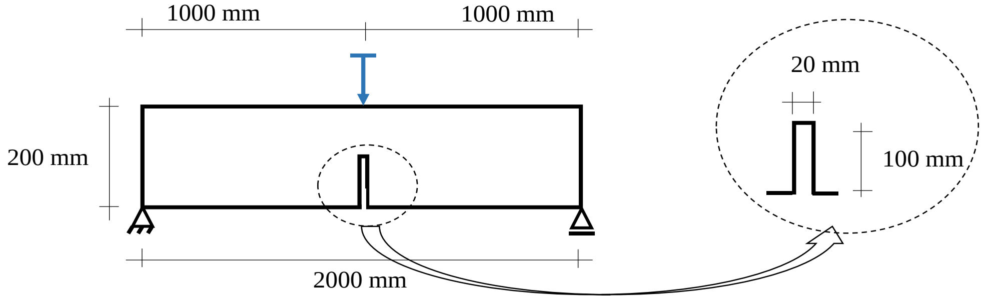

Figure 9: beam geometry and boundary conditions - three-point bending test.

Table 2. Meshes for the three-point bending test

Name	Total of elements	Elements at crack line
M1	381	15
M2	721	25
M3	811	25

Figure 10 shows the meshes used with discretization detail in the notched region.

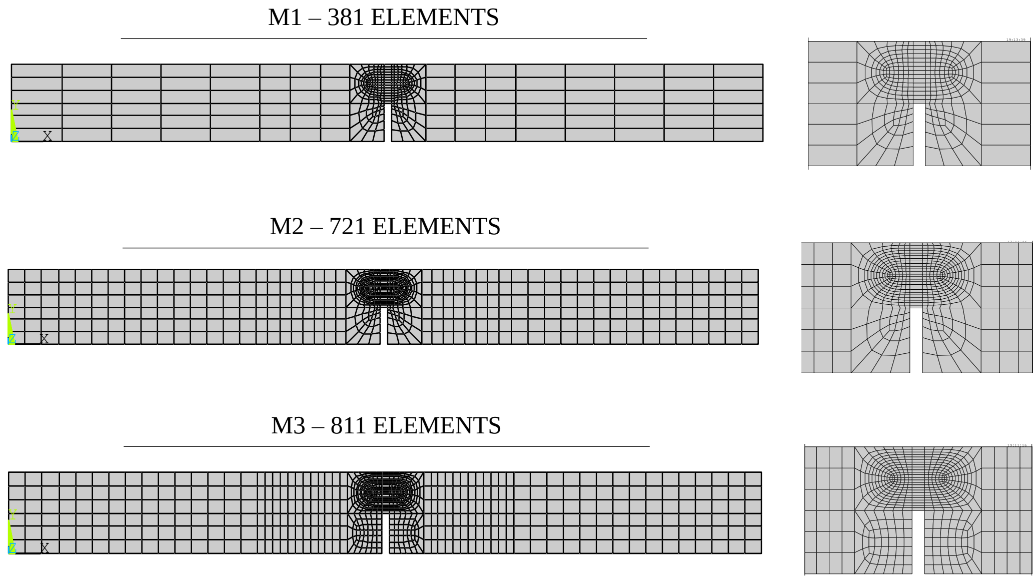

Figure 10: Discretization of the meshes with detail in the region of the notch - three-point bending test

Table 3 shows the input data used for this example and correspond to experiments done by Petersson (1981).

Table 3**.** Input parameters for three point bending test

Geometric Properties	
beam	
Length	2000 mm
Height	200 mm
Thickness	50 mm
Notch	
Length	20 mm
Height	100 mm
Thickness	50 mm
Material Properties	
Tensile strength (ft)	3.33 MPa
Young Modulus (E)	30000 MPa
Poisson coefficient (ν)	0.2
Fracture energy (Gf)	0.124 N/mm

Proceedings of the XXXVIII Iberian Latin-American Congress on Computational Methods in Engineering
P.O. Faria, R.H. Lopez, L.F.F. Miguel, W.J.S. Gomes, M. Noronha (Editores), ABMEC, Florianópolis, SC, Brazil, November 5-8, 2017.

For the non-cracked zone, a linear elastic constitutive relation was used. In the cracked zone, the influence of two different softening laws, one linear and one exponential, were presented in section 3.

Figure 11a) presents a comparison of the results obtained for the two softening laws used for the most refined mesh (M3) also the experimental results. As can be observed the exponential softening presents results very similar to the real behavior of the tested beam. In the linear model, the maximum stresses are overestimated and the post-peak curve is more brittle than the exponential model. According to Lens (2009), this brittle behavior for the linear model is due to the absence of fracture energy for larger openings, which are influenced by the aggregate interlock.

A comparison with different finite element meshes is presented in Figure 11b). It is noted that even for a coarse mesh (M1) the presented results are satisfactory and tend to converge to a smoother response with the refinement. It is important to emphasize that in the mesh generated the refinement of the cracked zone was prioritized.

a) b)

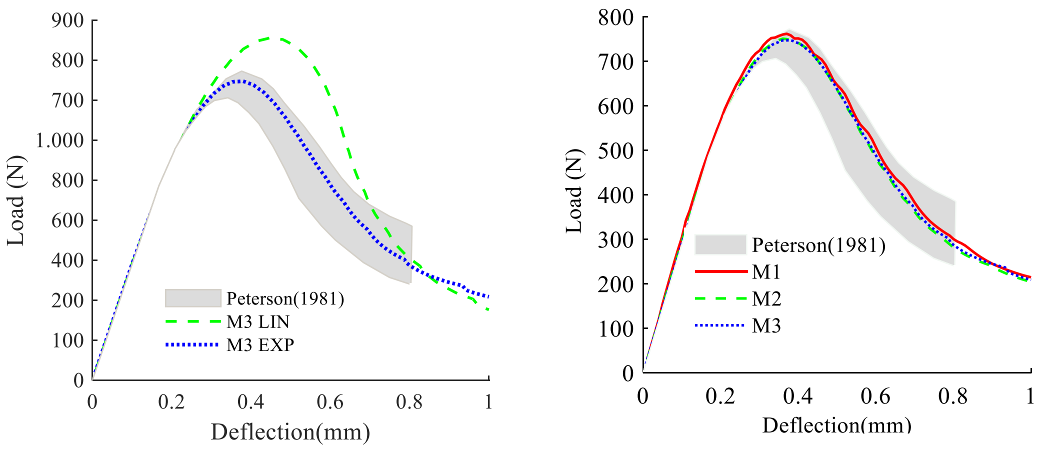

Figure 11: Load x Deflection of beam with softening. a) refined mesh – linear and exponential softening; b) different mesh sizes – exponential softening.

5 CONCLUSION

The aim of this work was to analyze the behavior of structural elements of simple concrete for different constitutive relations in the post-peak branch, using a model with strong discontinuities.

The implemented model was based on the model proposed by Dvorkin, Cuitiño and Gioia (1990), where a cracking model based on kinematically and statically optimal non-symmetric elements (SKON) formulation was implemented and used the QMIT finite element (Quadrilateral with Mixed Interpolation of Tensorial Components) was used. In this paper we propose the use of the quadrilateral bilinear element in addition to the use of the symmetrical part of the stiffness matrix.

It was possible to verify that the softening laws have big influence on the behavior of the structure. The exponential softening model (Dvorkin, Cuitiño, Gioia, 1990) appeared to be the best solution. In the pure tensile test we noticed that the exponential model presented a post-peak behavior similar to that observed in experimental analyzes. In the bending test using the exponential model the peak stress was correctly estimated and the softening curve presented a more realistic behavior in comparison with experimental data. In the linear model (Hillerborg, Modéer, Petersson, 1976), the maximum loads were overestimated when compared to experimental data, in addition, the linear model presented a more brittle softening branch than is actually observed for quasi-brittle materials. In general, the results obtained presented a good agreement to the experimental results as well as numerical results obtained by crack models presented in the literature.

Acknowledgment

The authors gratefully acknowledge the financial support provided by Brazilian Government through CNPq and CAPES.

REFERENCES

Araújo, J. M. de., 2001. *Estruturas de concreto - A resistência à tração e energia de fratura do concreto*. Dunas.

d'Avila, V. M. R., 2003. *Estudo sobre modelos de fissuração de peças de concreto armado via método dos elementos finitos*. Doctoral Thesis, Universidade Federal do Rio Grande do Sul/Porto Alegre.

D'hers, S., Dvorkin, E. N., 2008. Modelling of strain localization via a two-scale formulation. In Cardona, A., Storti M. & Zuppa, C., eds, *Mecánica Computacional Vol XXVII,*, vol. 28, pp. 1225–1236.

Driemeier, L., 1999. *Contribuição ao estudo da localização de deformações com modelos constitutivos de dano e plasticidade.* Doctoral thesis, Universidade de São Paulo/ São Carlos.

Dvorkin, E. N., Assanelli, A. P., 1991. 2D finite elements with displacement interpolated embedded localization lines: The analysis of fracture in frictional materials. *Computer Methods in Applied Mechanics and Engineering*, vol. 90, n. 1–3, pp. 829–844.

Dvorkin, E. N., Cuitiño, A. M.; Gioia, G., 1900. Finite elements with displacement interpolated embedded localization lines insensitive to mesh size and distortions. *International Journal for Numerical Methods in Engineering*, vol. 30, pp. 541–564.

Hillerborg, A., Modéer, M., Petersson, P.-E., 1977. Analysis of crack formation and crack growth in concrete by means of fracture mechanics and finite elements. *Cement and Concrete Research*, vol. 6, n. 6, pp. 773–781.

Hordijk, D. A., 1991. *Local approach to fatigue of concrete*. Doctoral Thesis, Delft University of Technology/TU Delft.

Jirásek, M., 2000. Comparative study on finite elements with embedded discontinuities. *Computer Methods in Applied Mechanics and Engineering*, vol. 188, n. 1–3, pp. 307–

330.

Lens, L. N., 2009. *Modelos para análise de fratura do concreto simples empregando interfaces coesivas*. Doctoral thesis, Universidade Federal do Rio Grande do Sul/ Porto Alegre.

Oliver, J., Huespe, A. E., Samaniego, E., 2003. A study on finite elements for capturing strong discontinuities. *International Journal for Numerical Methods in Engineering*, vol. 56, n. 14, pp. 2135–2161.

Petersson, P.E., 1981. Crack growth and development of fracture zones in plain concrete and similar materials. University of Lund/ Lund.

Silva, C. Z. da, 2015. *Uso de descontinuidades fortes na simulação de problemas de fratura.* Master dissertation, Universidade Federal do Rio Grande do Sul/Porto Alegre.

Spencer, B., 2000. *Embedded Crack elements for analysis of reinforced concrete*. PhD thesis proposal, University of Colorado/Colorado.

Van Vliet, M. R. A., Van Mier, J. G. M., 2000. Size Effect in Tensile Fracture of Concrete and Rock. *Heron*, vol. 45, n. 2, p. 91–108.